METHODS OF PARALLEL VOXEL MANIPULATION FOR 3D DIGITAL PRINTING

Jonathan Hiller, Hod Lipson
Mechanical and Aerospace Engineering
Cornell University
Ithaca NY, USA

Abstract

A novel digital printing concept is explored for desktop fabrication of multi-material objects with arbitrary 3D geometry. Digital objects are composed of many discrete, self-aligning voxels instead of continuous (analog) deposition techniques. Overall accuracy is determined by the individual voxels instead of the printer, and digital properties such as perfect replication and error correction are physically meaningful. The key challenge in digital printing is massively parallel, deterministic voxel manipulation. To quickly print millions of voxels while keeping errors low, we propose a parallel manufacturing process that exploits electrostatic forces to place an entire 2D pattern of voxels concurrently. Using a custom charged print head, we demonstrate selective 1.5mm voxel pick-up within a larger, self-aligned layer. We expect the principle to scale to million voxel layers using currently available technology.

Introduction

Digital materials, which are composed of many self aligned fundamental building units, offer advantages over conventional analog materials used in all current manufacturing processes. (Gershenfeld, 2005) Favorable properties found in the digital electronics domain such as perfectly repeatability and error correction are physically meaningful with digital materials. A digital fabricator (Popescu *et al*, 2006a) can create objects more dimensionally precise than its own positioning system, and in theory every voxel (a physical instantiation of a 3D pixel) is completely recyclable. This approach to fabrication is inspired from biology, wherein all life is made of a series of fundamental, aligned building blocks. DNA, proteins, and amino acids are all example of digital materials. Additionally, the transition from analog to digital technologies has revolutionized many fields such as computing, communications, printing, music and picture storage, etc. In general, this transition has dramatically increased the capability and availability of a technology while decreasing the cost in production.

Although conventional solid freeform fabricators typically use digitally controlled positioning systems, the material deposition itself is inherently analog. Thus, the finished part cannot be more precise than the digital positioning system and any subsequent measurements and replications will lose accuracy. Additionally, conventional freeform fabrication is often limited to a single, homogeneous material. (Kadekar *et al*, 2004) Multi-material FDM and inkjet fabrication machines are limited to a small subset of materials with very specific rheological properties (Malone *et al*, 2003; Calvert, 2001). We demonstrate the foundations for Digital Freeform Fabrication (DFF) technology

(Figure 1) that scales naturally to megavoxel structures while retaining control over the material of each individual voxel. The process is compatible with virtually any number and combination of materials that are solid at room temperature. Additionally, the overall error of a macroscale digital object scales favorably as the microscale random errors of each voxel tend to cancel out. (Hiller and Lipson, 2007)

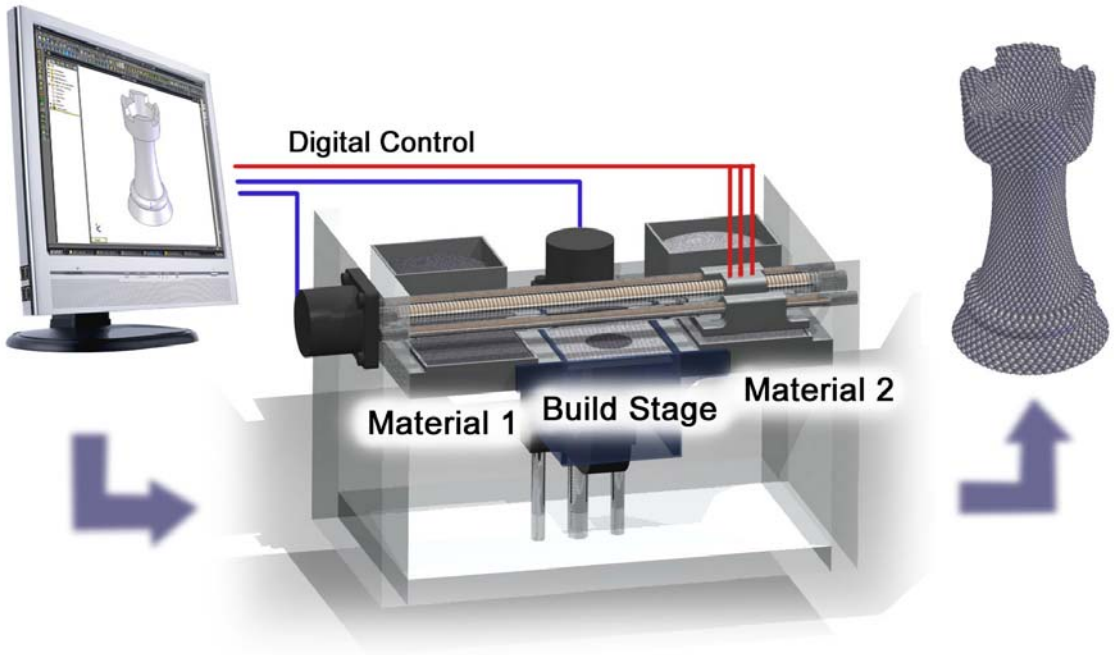

Figure 1: The concept of digital printing using build and support materials to create a function freeform 3D object.

In principle, a physical voxel must passively self-align with its neighbors while being conducive to parallel assembly and easy to make precisely in large quantities. We have explored a variety of voxel shapes that self align and even interlock (Hiller and Lipson, 2007) and ultimately chose spherical voxels. This is due to their simplicity and wide availability at all scales (Kawaguchi, 2000) in multiple materials at a low cost and high precision. Additionally, spheres have a high degree of self-alignment capability (Ye *et al*, 2001). A brief discussion of the theory behind electrostatic manipulation will be presented, followed by a detailed description of an electrostatic printhead. The core technical steps of a multilayer digital fabricator are then outlined, explained in detail, and demonstrated.

Background

A digital fabricator must quickly assemble objects composed of millions of voxels to have practical applications. This necessitates a massively parallel assembly process. The greatest technical challenge in digital manufacturing is to individually determine the presence and material type of each voxel within a large 3D matrix. This is accomplished most efficiently using a 2D parallel assembly process in which an entire layer of voxels of each material is placed at once. To address this technical challenge, we introduce a

hybrid idea of self assembly and top-down assembly to place arbitrary layers of voxels. Self assembly exploits the alignment properties of many identical elements to create ordered structures. (Whitesides and Gryzbowski, 2002) However, it is very difficult to program arbitrary shapes, as each individual element must have knowledge of the overall structure and its own location. However, top down assembly, which allows complete control over each voxel, (Popescu *et al*, 2006b) requires a prohibitive amount of effort to build structures with many thousands or millions of elements.

In our solution, the self alignment properties of the voxels are used to organize (self assemble) an entire, homogenous layer of voxels. Once complete, the relative location of each voxel within this 2D matrix in the pre-assembly area is known. This allows an indexed print head to come into contact with a single voxel at each cell location within its matrix, which it can either attract or not using a selective electrostatic charge as used in xerography.

Relative scales are important in order to effectively use electrostatic forces to manipulate voxels. (Figure 2) In this paper, we consider 1.5mm spherical voxels made of acrylic, although the analysis and results hold in principle for any non-conductive material. The analysis of voxels made of conductive material is similar but not presented here. At the millimeter scale, the magnitude of electrostatic forces on a sphere can be more than an order of magnitude greater than the gravitational force.

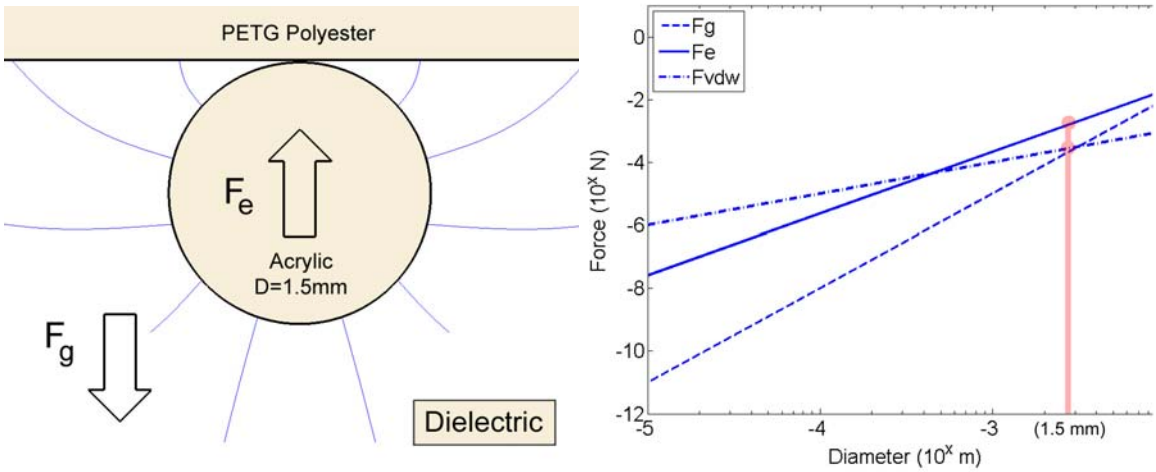

Figure 2: Electrostatic force F_e must be greater than gravitational force F_g to effectively manipulate a sphere (left) which is the case for 1.5mm spheres (right). Van der Waals force F_{vdw} may also aid attraction. (Figure at right adapted from Arai *et al, 1996*)

Results and Discussion

An electrostatic voxel deposition print head has been developed to selectively pick up voxels from a pre-aligned layer from above, lift them out, and deposit them on a build stage. (Figure 3) For these experiments, a layer consists of 55 voxels arranged within an equilateral triangular area, and the print head has the identical pattern of cells

that can attract a single voxel each. The print head consists of a voxel cell array, which maintains the relative positions of each voxel, the separation layer which may either insulate or conduct charge to the ground plane, the ground plane, and the rigid body for mounting the head to an X-Z stage. An insulative separation layer made of PETG polyester was used here.

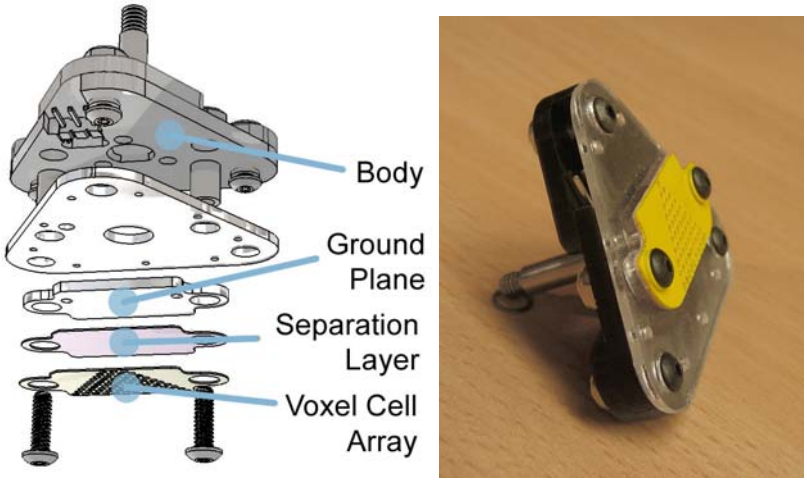

Figure 3: Exploded view of the electrostatic print head (left) and actual assembled view (right)

For this analysis, we will consider an insulating separation layer thick enough to reduce any effects of the mobile electrons in the ground plane. The problem of attractive force between a sphere (conducting or dielectric) and a plane (conducting or dielectric) has been well studied (Berry and Higginbotham, 1975; Xiaoping, 1987; Techaumnat and Takuma, 2006) In the case of our experiments, a dielectric voxel should be attracted to a semi-infinite dielectric plane, as studied by Jingyi and Xiaoping (1988).

To successfully lift a sphere, the attractive electrostatic attraction force between the sphere and the print head must be greater than the force that gravity and the print head acceleration can exert. Each 1.5mm diameter acrylic sphere weighs approximately 2.4mg. Under gravity and 1G opposing acceleration of the print head, 40μN of electrostatic force would be necessary to maintain contact with the print head. The attractive force between a sphere and a semi-infinite dielectric ground plane can be calculated approximately by solving the appropriate equation (Equation 1) for the given conditions (Jingyi and Xiaoping, 1988).

$$F = \int (\rho E_z - \frac{1}{2} E^2 \nabla \varepsilon) dv \qquad (1)$$

An electric field intensity of 72Kv/m was used for the calculations, coinciding with values measure during experimentation. Representative dielectric constants of 3.2 for the acrylic spheres, and 2.6 for the PETG separation layer were assumed, and the maximum surface charge density on the spheres in air of 26.5μC/m^2 was used. For the 1.5mm diameter spheres, the subsequent calculations yielded approximately 25μN of electrostatic force, which is less than the required 40μN. However, this does not account

for the nesting effect of the voxels within the cells of the print head, which has the effect of increasing the electrostatic attraction force due to more surface area of the sphere in close proximity to the head. Additionally, van der Waals forces may also contribute a measurable amount of attractive force. Combined, these effects could theoretically provide the necessary force to explain the observed experimental behavior. More detailed simulation will be necessary to confirm this. However, it is evident that spheres much larger than 1.5mm would be not well suited to electrostatic manipulation, whereas scaling the spheres down only increases the relative magnitude of the electrostatic force as compared to gravity.

A digital fabricator (Figure 4) is under development that is compatible with multi-material digital fabrication of thousands of voxels. This test bed has been used to demonstrate self aligning complete 2D layers and selectively picking up 1.5mm spherical voxels using electrostatic forces in a manner suitable to be integrated into a complete digital fabrication process.

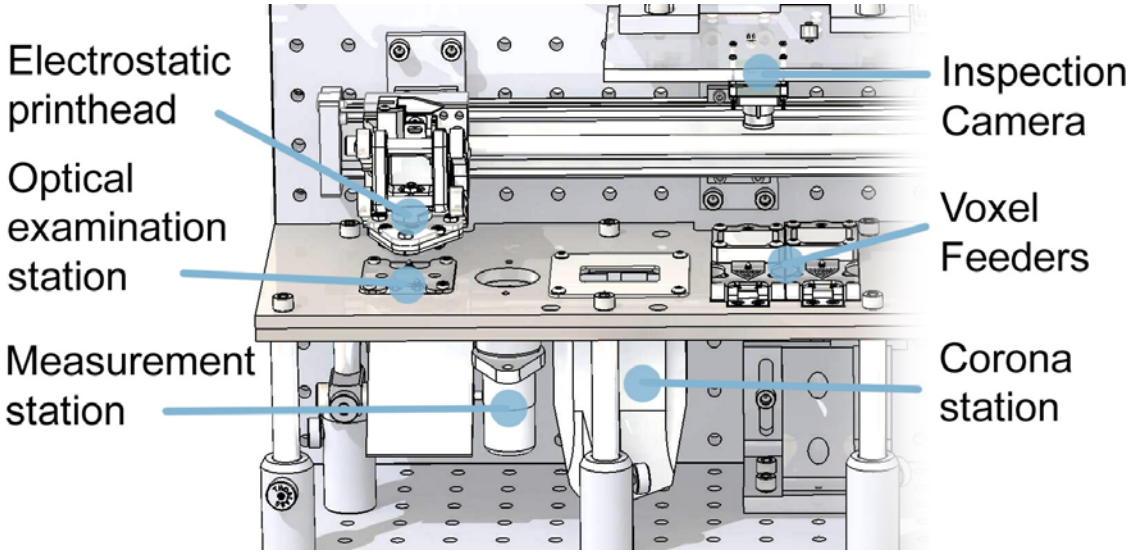

Figure 4: Schematic of digital fabrication experiment illustrating various stations in the build process.

A complete digital fabricator requires subsequent placing of many layers of different materials and the computation to calculate this. However, the main technological barriers that exist are addressed in the key steps of individual layer manipulation. The flow of electrostatic voxel manipulation for the digital fabrication process is as follows:

1) **Electrostatic charging:** The print head moves to the static charge station (Figure 5a) and a corona wire housed below emits a stream of ions to impart a static charge on the print head. To obtain a selective charge, a physical barrier was placed between the desired cells and the corona emitter.
2) **Layer self alignment:** Meanwhile, an entire layer of voxels is self aligned in the voxel feeder (Figure 5b) using gravity and vibration.

3) **Selective parallel voxel pickup:** The electrostatic print head moves over the appropriate voxel feeder and presses down uniformly on all voxels. (Figure 5c) When it lifts up, the voxels corresponding to the charged cells are carried along.

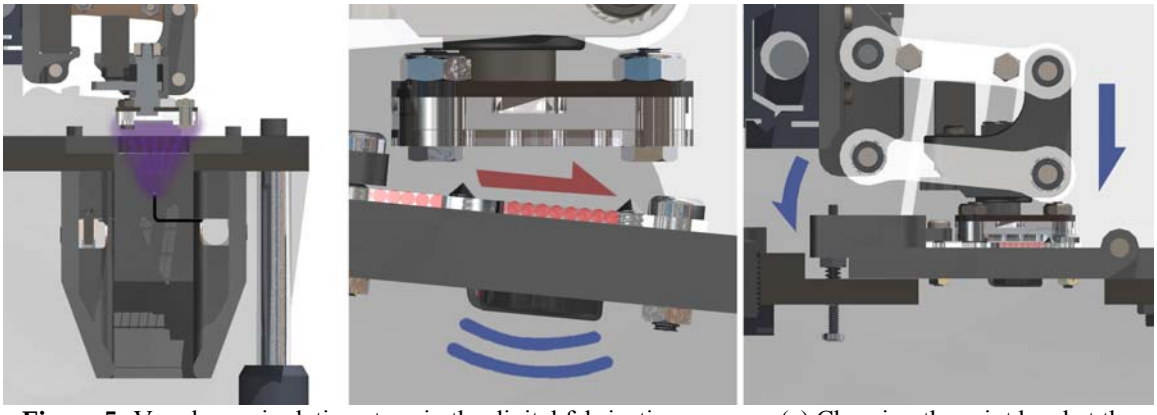

Figure 5: Voxels manipulation steps in the digital fabrication process. (a) Charging the print head at the corona station, (b) aligning a layer of voxels in the feeder, and (c) picking up a layer of voxels.

Each of these three steps is analyzed in detail below. This process requires a series of stations that the electrostatic print head must move between in order to complete the layer deposition process. (Figure 4) The print head moves between these stations on a linear stage with 300mm of travel at a maximum speed of 150mm/sec. The end effector incorporates an additional degree of freedom in the vertical direction, and is designed to lift the print head up while maintaining its horizontal orientation. The corona station houses the high voltage corona discharge system, and is insulated from its surrounding by an ABS plastic casing approximately 3mm thick. Another station houses a voxel feeder, where the voxels are picked up. Cone-headed indexing pins with adjustable height are present at each critical station that precisely align with indexing holes on the head as it presses down, ensuring accurate positioning.

A separate station houses a static electricity meter (Ultrastable Stable Voltmeter, Alphalab Inc., 0-20Kv range). Although not in the normal build sequence, this station was used extensively to obtain data on the relative charge of the print head by measuring the electric field emitted by it. When measuring a non-conductive surface, this particular sensor outputs a number proportional to the emitted electric field. Since the electrostatic print head does not fill the entire sensing field of view, a ground plane was introduced to mask any unwanted measurements. The electric field due to the print head was then calculated by dividing the total sensor measurement by the percent area of the print head. All subsequent data on the charge of the print head is presented in terms of the emitted electric field.

Electrostatic charging

In the first step of the layer deposition process, a corona wire is used to impart a static charge on the print head surface. Corona discharge occurs when the strength of an electric field increases to the point where the surrounding air is ionized, but an arc does not yet form. To obtain this in practice, a bare conductor in the shape of a needle is charged to high voltage, pointing upwards towards the print head. The ions that form at

the end of the needle are then attracted to a ground plane, drawing them up towards the print head. Although other methods exist to obtain a high static charge, such as triboelectric effects, corona discharge was selected to obtain a uniform static charge on a wide variety of materials.

A 35Kv DC voltage source using a Cockcroft Walton voltage multiplier (capacitor ladder) was used to power the corona wire with a maximum current of 1.5mA. In these experiments, the open circuit (no load) voltage of the ion emitter tip was varied between 6 and 9 Kilovolts. This alone is enough to ionize the surrounding air, but a flow of ions is set up in the presence of the ground plane housed in the print head, causing a net migration of charge through the air. If a non-conducting surface such as the separation layer is placed in this ionic wind, a static charge will be imparted on it. As the voltage per unit distance rises, the air begins to break down and conduct increasingly more charge until the point of arcing, which is to be avoided.

A series of experiments were conducted to characterize the charging process of the electrostatic print head. Variables we considered include the voltage of the corona wire, the distance between the emitter tip and the print head, and the time of charging. Other variables that were not considered include the geometry of the corona emitter tip, the thickness of the separation layer, and the ground plane resistance, which were held constant for this analysis. A positive relationship was observed between the emitter tip distance and resulting static charge on the print head, as shown in Figure 6 for a variety of corona voltages. This distance was measured from the tip of the emitter to the bottom plane of the print head. The exposure time was held constant at one second. This relationship can be explained by noting that as the corona tip approaches the print head, the voltage per distance rises. This allows the air to break down and conduct a greater amount, thus lowering the difference in potential, results in less charge on the head.

A positive relationship is also observed between the time the corona wire is emitting and the amount of static charge resulting on the head. (Figure 6) This is plotted on a logarithmic scale with exposure time varying from 25ms to 5 seconds. However, the maximum charge levels off very quickly as exposure time increases, and there are no significant gains in the measured electric field of the head after approximately one second of exposure.

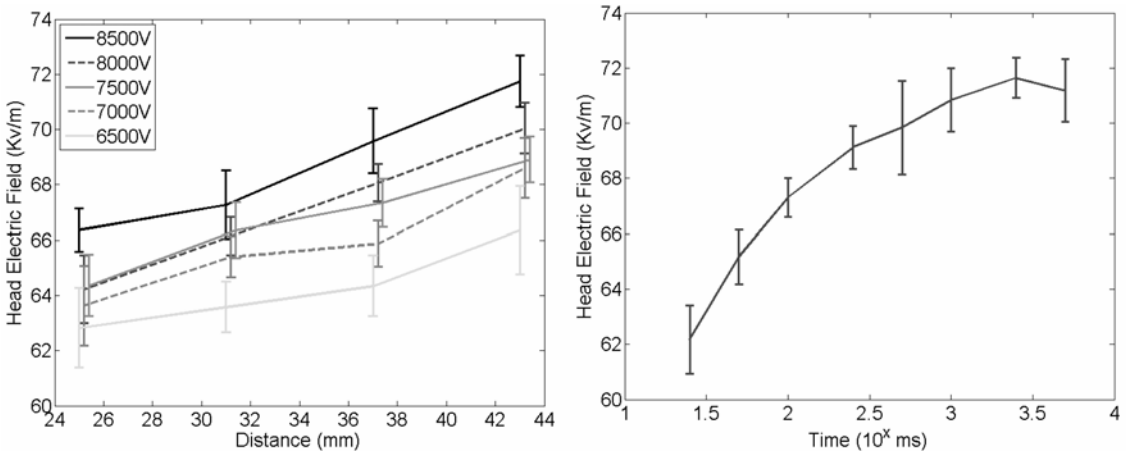

Figure 6: (a) Print head charge as a function of corona emitter distance for several corona voltages (left). (b) Print head charge as a function of corona exposure time.

Voxel layer self-alignment

The key to the massively parallel assembly process is the ability to selectively pick up voxels at arbitrary locations within a pre-aligned layer. In order to accomplish this, an entire layer of voxels is self aligned using gravity and vibration. Figure 7 shows frames from a video taken from above capturing the self alignment of the spheres. This process is highly repeatable and suitable for unsupervised automation. For this demonstration, a simple five second pulsed vibration pattern was programmed. However, with a suitable camera in place, it is a trivial machine vision problem to track the location of each sphere for closed loop feedback, resulting in a more robust self-organization process.

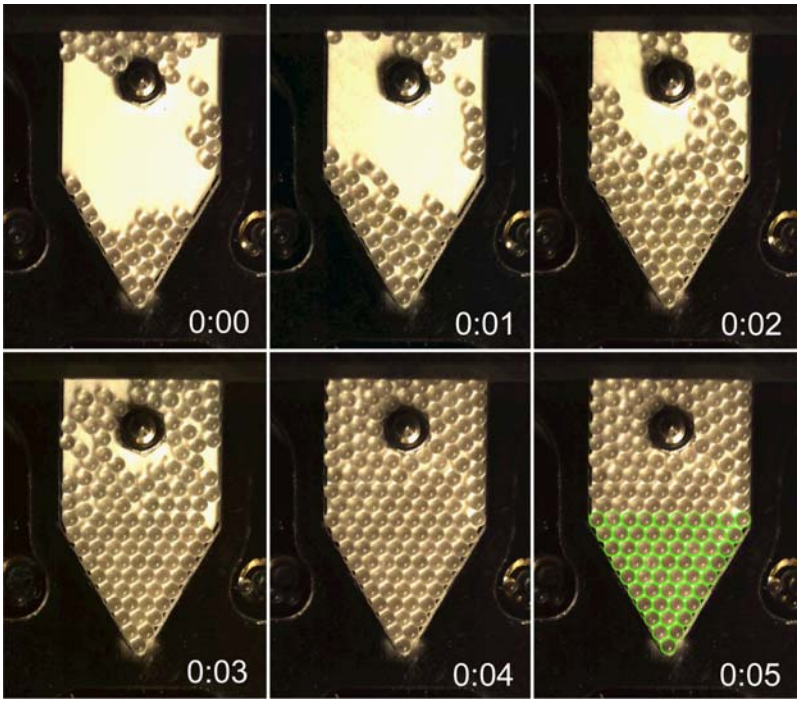

Figure 7: Frames from a video showing a layer of voxels self aligning in the feeder. Last frame shows a possible machine vision feedback result.

This process is effective with the voxel feeder spring-loaded to an inclination of only 2.5° (Figure 8). The voxel feeder was designed to hold a large number of voxels, and continually replenish the active layer as voxels are removed by the print head. A rotational stiffness of the voxel feeder of 30N-mm/degree was found to be sufficiently stiff to incline it at the desired angle for settling while being compliant enough to be pushed flat under the 360N-mm downward moment the print head can exert on the feeder. A 4mm diameter pager motor controlled by PWM provides more than sufficient vibration to break the static friction and allow the spheres to settle into place.

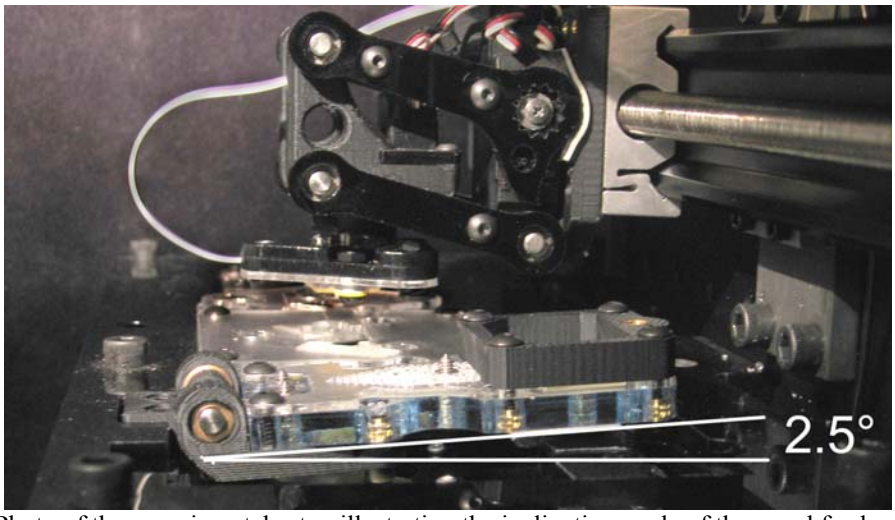

Figure 8: Photo of the experimental setup illustrating the inclination angle of the voxel feeder to align the spheres. The print head is also clearly visible.

Selective parallel voxel pickup

To demonstrate selective parallel voxel pickup, we first demonstrated full layer pickup using the electrostatic print head. Figure 9 shows three frames from a movie as the print head moves over, presses down, and lifts up with the majority (all but one) of the spheres. The camera was located below the voxel feeder pointing upwards, and the spheres are seen through its transparent bottom. This trial used a contoured print head interface consisting of five laser-cut layers with contours that fit each sphere in order to increase the surface area of the sphere-head interface.

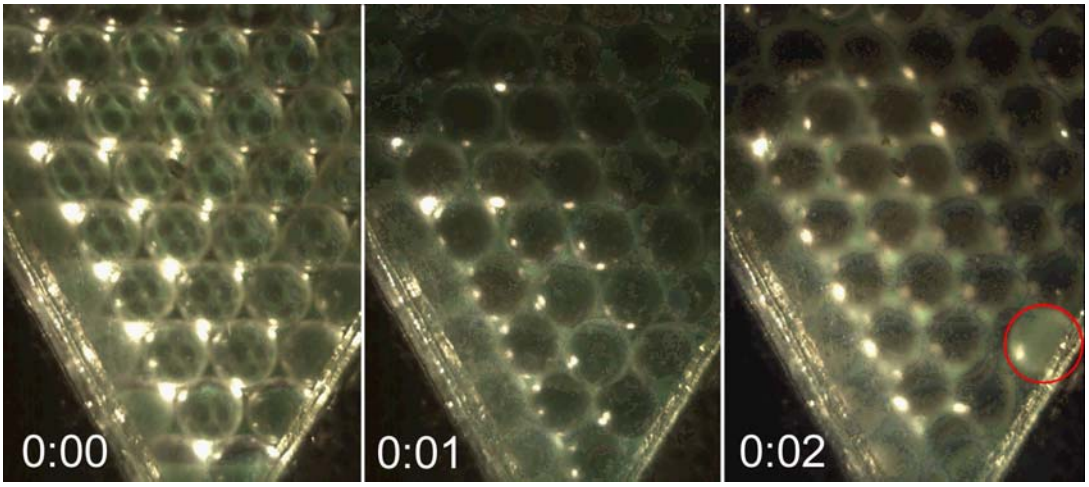

Figure 9: Electrostatic voxel pickup using 1.5mm acrylic spheres, viewed from below. Print head moves over aligned voxels (left), presses down (center) and lifts up all voxels except one (right, circled). The out-of-focus spheres have been lifted up from the feeder away from the camera.

However, not every sphere that was initially lifted from feeder stayed attached as the head moved away. This can be attributed to relatively harsh accelerations and vibrations from the stepper-motor driven X stage, as well as the static charge bleeding off to the surrounding air in the presence of humidity. For a relative humidity of 45%, a representative electrostatic discharge curve is shown in Figure 10. The experimental time constant is approximately 13 seconds. Given the time to place a layer is less than 3 seconds, and the most extreme forces are felt at the beginning of this, we are optimistic that this effect can be accounted for.

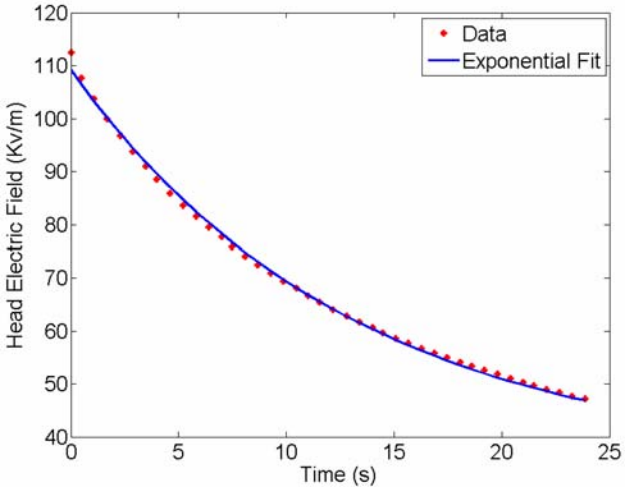

Figure 10: Relative charge loss of print head as a function of time. Experimental time constant is 13 seconds.

Next, custom masks were made for the corona charging station to physically block the charge from selected cells. A separate mask was made to block each half of the 55 cell triangle. Ten trial runs were done for each case. The number of voxels suspended in place on each half of the print head was recorded *after* it moved away from the feeder station (Figure 11). It was observed that a sphere was never erroneously deposited from

an uncharged cell. Within the charged region, the number of remaining spheres was consistently less than the total possible 25 cell locations, although still a significant percentage.

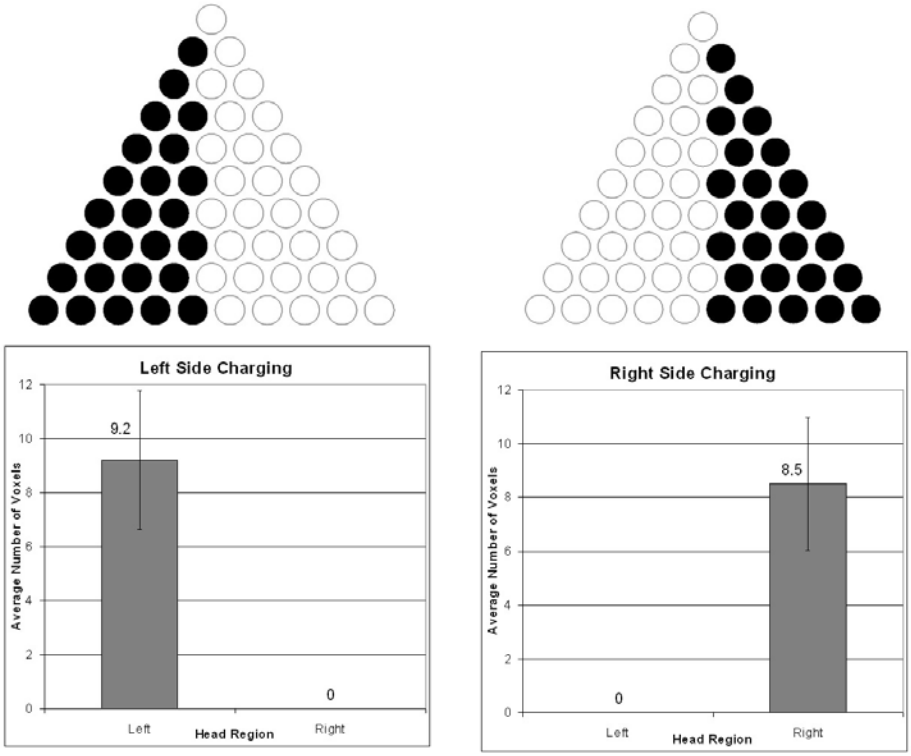

Figure 11: Results of voxel pickup experiment demonstrate selective manipulation

Conclusions

We have demonstrated the feasibility of selectively manipulating 1.5mm spherical voxels using electrostatic forces within a desktop experimental digital fabricator. All aspects of these experiments are designed to be parallel in nature and scale effortlessly to layers with arbitrarily large numbers of voxels. Thus, this research forms the technical foundation for a digital 3D printer capable of creating multi-material structures with millions of voxels.

Future work involves refining the experimental conditions and parameters such that individual voxels can be addressed and manipulated robustly. The separation layer will be switched to photosensitive material, such that the entire print head may be uniformly charged, then moved to an optics station where unwanted voxel locations are exposed to light from a scanning laser or computer projector. This allows the static charge to bleed to the ground plane behind, allowing for any arbitrary layer of voxels to be picked up within the output resolution of modern computers. The photosensitive material can also be uniformly illuminated in order to release the voxels once they have been stacked on the 3D assembly stage. Additionally, post processing techniques such as sintering will be examined to create rigid, functional 3D parts.

This work was supported in part by U.S. Defense Advanced Research Projects Agency (DARPA) project #W911NF-07-1-0298 and by a U.S. National Science Foundation (NSF) Graduate Student Fellowship.

References

1. Arai, F., Andou, D., Fukada, T., (1996)"Adhesion Forces Reduction for Micro Manipulation Based on Micro Physics", IEEE MEMS 6/1996, pp. 354-359
2. Berry, J., Higginbotham, I., (1975) "Electrostatic forces on a conducting sphere due to a charged, insulating plane", J. Phys. A: Math. Gen., Vol. 8, No. 11, pp. 1842-1851.
3. Calvert, P., (2001) "Inkjet Printing for Materials and Devices", Chemistry of Materials, Vol. 13, pp. 3299-3305.
4. Feng, J., Hays, D., (1998) "A Finite-Element Analysis of the Electrostatic Force on a Uniformly Charged Dielectric Sphere Resting on a Dielectric-Coated Electrode in a Detaching Electric Field", IEEE Transactions on Industry Apllications, Vol. 34, No. 1, pp. 84-91.
5. Gershenfeld, N., (2005) "Bits and Atoms", IS&T's NIP21: International Conference on Digital Printing Technologies, Baltimore, MD, Sept 2005, p. 2-2
6. Hiller, J., Lipson, H., (2007) "Design and analysis of digital materials for voxel-based 3D Printing", *Submitted for publication June 2007*
7. Jingyi, L., Xiaoping, C., (1988) "Electrostatic Problem of the System Consisting of a Dielectric Sphere and a Semi-Infinite Dielectric", IEEE 1988, pp. 1733-1734
8. Kadekar, V., Fang, W., Liou, F., (2004) "Deposition Technologies for Micromanufacturing: A Review", ASME Journal of Manufacturing Science and Engineering, Vol. 126, pp. 787-795
9. Kawaguchi, H., (2000) "Functional polymer microspheres", Progess in Polymer Science 25, pp. 1171-1210
10. Malone E., Rasa K., Cohen D.L., Isaacson T, Lashley H., Lipson H., (2003) "Freeform fabrication of 3D zinc-air batteries and functional electro-mechanical assemblies", Rapid Prototyping Journal, Vol. 10, No. 1, 2003, pp. 58-69.
11. Popescu, G., Kunzler, p., Gershenfeld, N., (2006a) "Digital Printing of Digital Materials", Int. conf. on Digital Fabrication Technologies, Denver Colorado, September 2006.
12. Popescu, G., Gershenfeld, N., Marhale, T., (2006b) "Digital Materials for Digital Printing", International conference on Digital Fabrication Technologies, Denver Colorado, September 2006.
13. Techaumnat, B., Takuma, T., (2006) "Analysis of the Electric Field and Force in an Arrangement of a Conducting Sphere and a Plane Electrode with a Dielectric Barrier", IEEE Transactions on Dielectrics and Electrical Insulation Vol. 13, No. 1, pp. 336-344.
14. Whitesides, G., Gryzbowski, B., (2002) "Self Assembly at All Scales", Science, Vol. 295, pp. 2418-2421, March 2002.
15. Xiaoping, C., (1987), "Surface Charge Density of a Dielectric particle Near a Plane", J. Electrostatics, Vol 20, p. 239.
16. Ye, Y.-H., Badilescu, S., Truong, V., Rochon, P, Natansohn, A., (2001) "Self-assembly of colloidal spheres on patterned substrates", Applied Physics Letters, Vol. 79, No. 6, pp. 872-874